ISIJ International, Vol. 56 (2016), No. 9, pp. 1668–1674

Hardening Optimization of High Chromium-manganese Austenitic Steel

Silvia BARELLA,[1)] Carlo CENA,[1)] Andrea GRUTTADAURIA,[1)] Carlo MAPELLI,[1)]* Davide MOMBELLI,[1)] Dario RIPAMONTI,[2)] Giovanni FANTINI[3)] and Daniele DIONI[3)]

1) Sezione Materiali per Applicazioni Meccaniche, Dipartimento di Meccanica – Politecnico di Milano, via La Masa 1, 20156 Milano, Italy. 2) National Research Council, CNR - Institute of Condensed Matter Chemistry and Technologies for Energies, ICMATE (CNR-IENI), via Roberto Cozzi 53, 20125 Milano, Italy. 3) M&M Forgings S.r.l., via degli Emigranti 5, 25040 Cividate Camuno, Italy.

(*Received on March 8, 2016; accepted on May 17, 2016*)

The study is focused on the assessment of the best thermal range for plastic deformation of Cr–Mn austenitic steel, to obtain a correct hardening and mechanical properties at room temperature. This steel grade is featured by a fully austenitic microstructure deriving from the high concentration of Mn and N, and is mainly used for the retaining rings bearing of power generation shafts. These components should not have magnetic permeability and thus, the mechanical strengthening can be performed by strain hardening and activation of twinning systems during rolling and forging at high temperature. Different specimens were tensile tested at different temperatures and different strains without arriving at the fracture point. Once the strained specimens were cooled, they have been tested by complete tensile tests at room temperature to determine the final mechanical properties. The best combination of the final mechanical properties have been obtained for plastic deformation performed between 250°C and 350°C, but the formation of martensite at 250°C narrows the useful thermal range between 300°C and 350°C. The metallographic observations indicated that the best hardening conditions can be obtained through the exploitation of the twinning plasticity effect and when the deformation temperature avoids any recovery that can reduce the dislocation density maintained after the cooling at room temperature. The performed experimental trials have also allowed stating the most favorable thermal range for the strain hardening of Cr–Mn steels through forging process to maximize the strengthening effect without the detrimental chromium carbide precipitation.

KEY WORDS: austenite; plastic deformation; manganese; twinning; hardening.

1. Introduction

The interesting properties of austenitic Fe–Mn–C steels were originally discovered and exploited by Sir Robert Hadfield in the late nineteenth century.[1)] The most used austenitic stainless steels are featured by low carbon concentrations and nickel is used to stabilize the face centered cubic (fcc) elementary cells, but the same austenite stability is obtained by replacing nickel with manganese and carbon which are cheaper than nickel and they allow obtaining the highest final mechanical performances often required by the specifications. When the carbon concentration of the Hadfield steel cannot be used, because such a high carbon concentration (*i.e.* 1.2%wt.) implies a very poor weldability, and high strength of steel is needed, the simultaneous stabilization of the austenite and the high strength are obtained by addition of manganese and chromium.[2–4)] The manganese concentration has to be set at values higher than 15%wt. and the nitrogen concentration is usually maintained higher than 0.5%wt. because such a chemical composition is able to avoid an abundant $\gamma \rightarrow \alpha'/\varepsilon$ (austenite→martensite) transformation during the plastic deformation process. Actually, the plastic deformation of an austenitic stainless steel can lead to a phase transformation from a paramagnetic austenite to a ferromagnetic martensite that is not allowed for the application in which the time-variant electromagnetic fields are involved, otherwise the heating and/or a Lorentz force can be developed within the mechanical component and this can compromise the mechanical stability.[5–7)]

This study aims at finding the best hardening temperature for X10CrMnN18-18 (**Table 1**) featured by a fully austenitic micro-structure (**Fig. 1**(a)), in order to provide the maximum increase of the mechanical properties, to avoid the formation of the martensite (Fig. 1(b)), to make the plastic deformation possible and to induce the desired hardening.

Such steel is often used to obtain retaining rings (**Fig. 2**) for the power generation shaft. These mechanical components can be interested by the magnetic flow of the rotating magnet belonging to the alternator, but at the same time they have to assure mechanical properties able to provide the safe working conditions (**Table 2**).

The strengthening mechanism of the studied steel relies on the strain hardening and on the substitutional solu-

* Corresponding author: E-mail: carlo.mapelli@polimi.it
DOI: http://dx.doi.org/10.2355/isijinternational.ISIJINT-2016-135

Table 1. Chemical composition of the austenitic steel X10CrMnN18-18.

Element	C	Mn	Si	P	S	Cr	Ni	Mo	Cu	V	Al	N
%wt	0.09	19.5	0.55	0.02	0.002	18	0.82	0.3	0.08	0.11	0.015	0.56

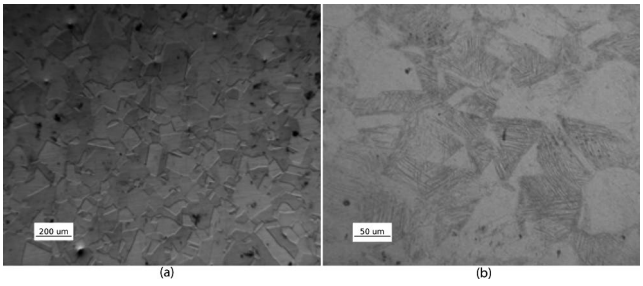

Fig. 1. Austenite matrix of X10CrMnN18-18 at room temperature (a) and structure formed by the deformation at room temperature (b): grains of austenite (brigth) and α' martensite (dark grains).

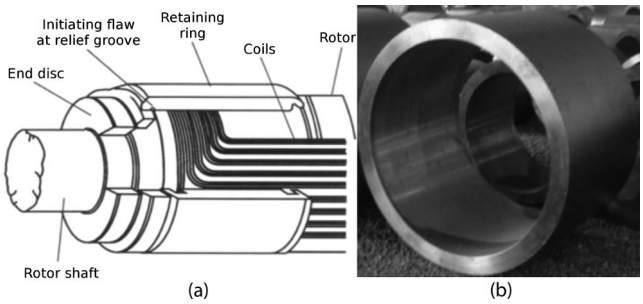

Fig. 2. Scheme about the retaining rings use (a) and an example of a forged retaining ring (b).

tion performed by the presence of chromium. The strain hardening is achieved by plastic deformation,[1,8] because the absence of any structural transformation induced by a thermal treatment excludes the possibility to realize any strengthening by the application of a heat treatment. The high chromium concentration is not only imposed to assure a good resistance against the oxidation and wear, but also to realize the hardening by the substitutional solution mechanism exploiting the strengthening phenomenon defined as the "Suzuki" effect.[9] The latest takes place in γ-Fe austenitic steels, where the dislocations are dissociated. The stacking sequence in the regions of the stacking fault between two partial dislocations is a thin region featured by a hexagonal compact prism (hcp) elementary cells. The solubility of the alloying elements may be higher in the stacking fault than in the bulk lattice and as a consequence the solutes can segregate to the region interested by the stacking fault, so they can immobilize the partial dislocations. On the other hand, the presence of so high chromium concentration could cause a detrimental precipitation of the chromium carbides that has to be avoided in order to exclude an undesirable hot shortness phenomenon, which cannot allow the exploitation of the desired hardening mechanism.

The aim of the performed study is the definition of the most favorable temperature for performing the strain hardening process of the studied steels in order to maximize the strengthening of the steel and to avoid the damages of such an alloy. It is demonstrated that the high temperature

Table 2. Usual minimal mechanical requirements for the application of austenitic steel X10CrMnN18-18 (UTS: ultimate tensile stress, YS: yield, A%: total elongation, Z% reduction area).

UTS [MPa]	YS [MPa]	%A	%Z
> 1 150	> 1 128	> 15	> 53

ranges (450°C–500°C) usually imposed by the forgemasters do not represent the most reliable conditions and that the lower temperature ranges can represent a more efficient and safe option.

2. Experimental Procedure

A 5t ingot in X10CrMnN18-18 steel has been degased and cast by bottom pouring. The steel has been forged between 1 050°C and 950°C to obtain a 300 mm diameter bar that has been air cooled down to room temperature. At 7.5 mm from the surface the material has been sampled to obtain tensile specimens whose axis is parallel to the forged bar main axis. The round tensile specimens are 8 mm in diameter and the parallel gauge length is 100 mm. The tensile specimens have been strained at 2 mm/min by a tensile machine equipped by a resistance insulated furnace controlled by thermo-couple and these specimens have been strained up to fracture at different temperature: 250°C/300 °C/350°C/400°C/450°C/500°C. Three specimens for each temperature have been tested. Once the complete stress vs. strain curves has been obtained for each plastic deformation temperature, the specimens have undergone a tensile test at the same temperatures up to 23% deformation and after such a plastic deformation they have been quenched in liquid nitrogen to freeze the microstructure condition formed at high temperature. A deformation limit of 23% deformation has been stated in order allow examination of the same deformation level for all the investigated temperature applied for the tensile strength, because there is a maximum elongation limit of 24% for the tensile test performed at 500°C. Then, the quenched specimens have undergone a tensile test at room temperature up to the fracture in order to point out the obtained mechanical properties as a function of the applied hardening temperature. The round specimens are 7 mm in diameter and 130 mm long. The test were conducted using a 50 mm gauge length extensometer and the crosshead speed was 10 mm/min.

A metallographic analysis has been carried out on the quenched specimens before the final tensile tests at room temperature. The observation of the microstructure before the final tensile tests aims at relating the microstructure obtained after the straining at high temperature with the mechanical properties measured by the tensile tests performed at room temperature. The sections of the tensile specimens have been observed along the transverse and longitudinal sections and they have been electrochemically

etched by oxalic acid (solution 10%, 15 V).

SEM-EBSD investigations have been performed to point out the difference of the crystallographic orientation after the deformation realized at different temperatures, because the data about the crystal orientation can be coupled with the grain size measurement and they can provide information about the possible microstructural reorganization phenomena (*i.e.* recovery, grain growth *etc.*) undergone by the steel that can affect the final mechanical properties. Moreover, the misorientation measurements allow recognizing the fraction of the special CSL (Coincident Site Lattice) boundaries, because Σ3 boundaries are associated to the presence of the twinnings.

High resolution metallographic investigations were performed by means of electron microscopy SU-70 by Hitachi, equipped with STEM detector and with a field emission Schottky electron source. The beam can be accelerated up to 30 kV. Thin foils for STEM observations were prepared by electro-etching 3 mm diameter large and 80–100 μm thick discs, obtained via mechanical polishing. The final perforation was performed by an electrolytic cell equipped with a double jet system, using a 59% methanol - 35% butanol - 6% perchloric acid solution, at a temperature of −30°C, operating at an applied voltage to induce a current of 0.1 A. The dislocation density has been measured by a linear intercept method applied on the STEM micrographs.

The presence of martensite has been checked at room temperature through the measurements performed by a ferritoscope on the specimens plastically strained at different temperatures, while the volume fraction of the chromium carbides has been pointed out through the optical microscopy observation and the detection of the dark phases on the grain boundaries has been performed by an automatic image analyzer.

3. Results

The ferritoscope has pointed out the presence of 23% volume fraction of martensite only in the specimens plastically deformed at 250°C, while the specimens deformed at the other temperatures have not point out any magnetic permeability, so the presence of martensite has to be excluded. The complete tensile tests at high temperature point out

Table 3. Mechanical properties measured during the high temperature tests.

Temperature [°C]	FS [MPa]	UTS [MPa]	%A	%Z	n
250	285	627	38	68	0.38
300	279	667	44	67	0.4
350	274	641	38	69	0.38
400	268	611	37	67	0.37
450	245	573	32	68	0.36
500	225	513	24	38	0.26

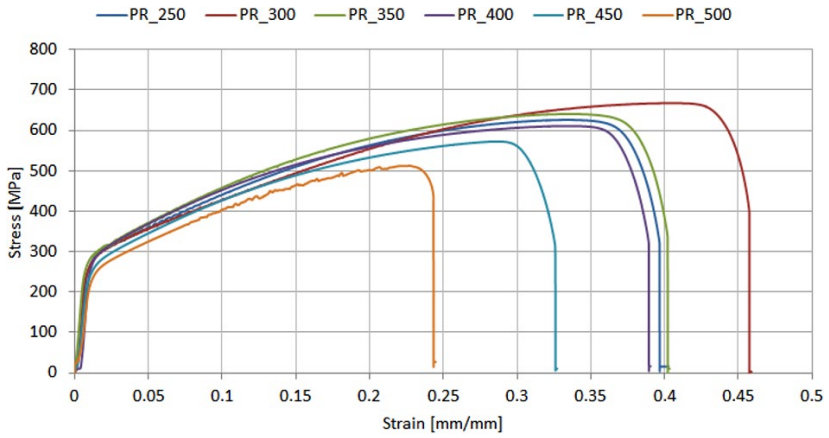

Fig. 3. Stress-strain curve at high temperature. (Online version in color.)

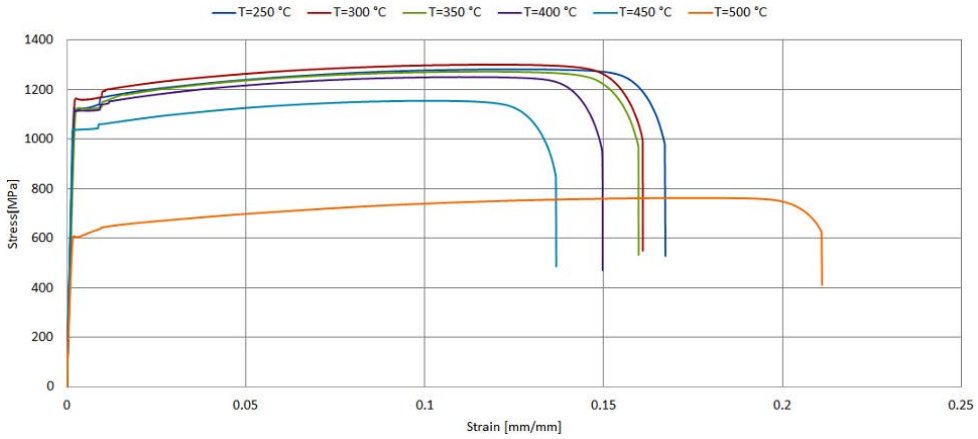

Fig. 4. Tensile test performed at room temperature after the deformation up to 23% of the overall elongation as a function of the different applied temperature. (Online version in color.)

a significant decrease of the ductility as the temperature increases, which is very sharp at the highest tested temperature (500°C) (**Fig. 3**). The best ductility properties are associated to a deformation temperature included between 250°C and 400°C that allows obtaining a percentage elongation peak up to 44% observed at 300°C. The Flow Stress (FS) measured at different temperature is not interested by significant difference as a function of the temperature increase but the difference is concentrated in the values of the Ultimate Tensile Strength (UTS), Elongation (%A) and in the Hardening Coefficient (n) (**Table 3**) according to the Hollomon relation usually applied to describe the constitutive law of an alloy during the plastic deformation (Eq. (1)):

$$\sigma = k\varepsilon^n \quad \text{..... (1)}$$

The different microstructures induced through the application of a different plastic deformation temperature cause a different mechanical behavior at room temperature. Actually, the specimens hardened by a straining up to 23% point out a significant variation of the mechanical behavior as a function of the formerly applied temperature (**Fig. 4**, **Table 4**).

A very sharp change of the mechanical behavior at room temperature is shown for the samples hardened at 450°C and 500°C that are featured by a lower yield strength than the specimens strained at a lower temperature, while the highest ductility is pointed out by the specimen plastically deformed at 500°C. The strain aging phenomenon disappears completely at room temperature after a plastic straining at 500°C.

The metallographic observations performed after the fracture at high temperature (**Fig. 5**) points out that the plastic deformation has occurred by twinning that is particularly intense and evident for the specimens plastically deformed at 250°C, 300°C and 350°C. The specimens deformed at the lowest temperature (250°C) are the only ones pointing out the presence of martensite, while all the other specimens tested at a higher temperature are not interested by the formation of this structural constituent. In the coupons tested at 300°C and 350°C a significant presence of twinning has taken place, but as the temperature increases further (400°C/450°C) the twinning density decreases and at 500°C the twinning formation decreases to a very low percentage fraction and the grains are surrounded by a significant presence of the precipitates **Table 5**. The misorientation measurements confirm the decrease of the twinning density as the applied deformation temperature increases, actually the fraction of Σ3 boundaries decreases as the applied plastic deformation temperature increases (**Fig. 6**). The SEM-EDS analysis has allowed identifying such precipitates as chro-

Table 4. Mechanical properties at room temperature revealed on the specimens previously treated at different temperatures.

Treatment Temperature [°C]	Yield Strength [MPa]	UTS [MPa]	%A	%Z
250	1 168	1 238	17	55
300	1 199	1 258	16	56
350	1 178	1 225	16	55
400	1 152	1 221	15	54
450	1 053	1 127	14	53
500	610	762	21	29

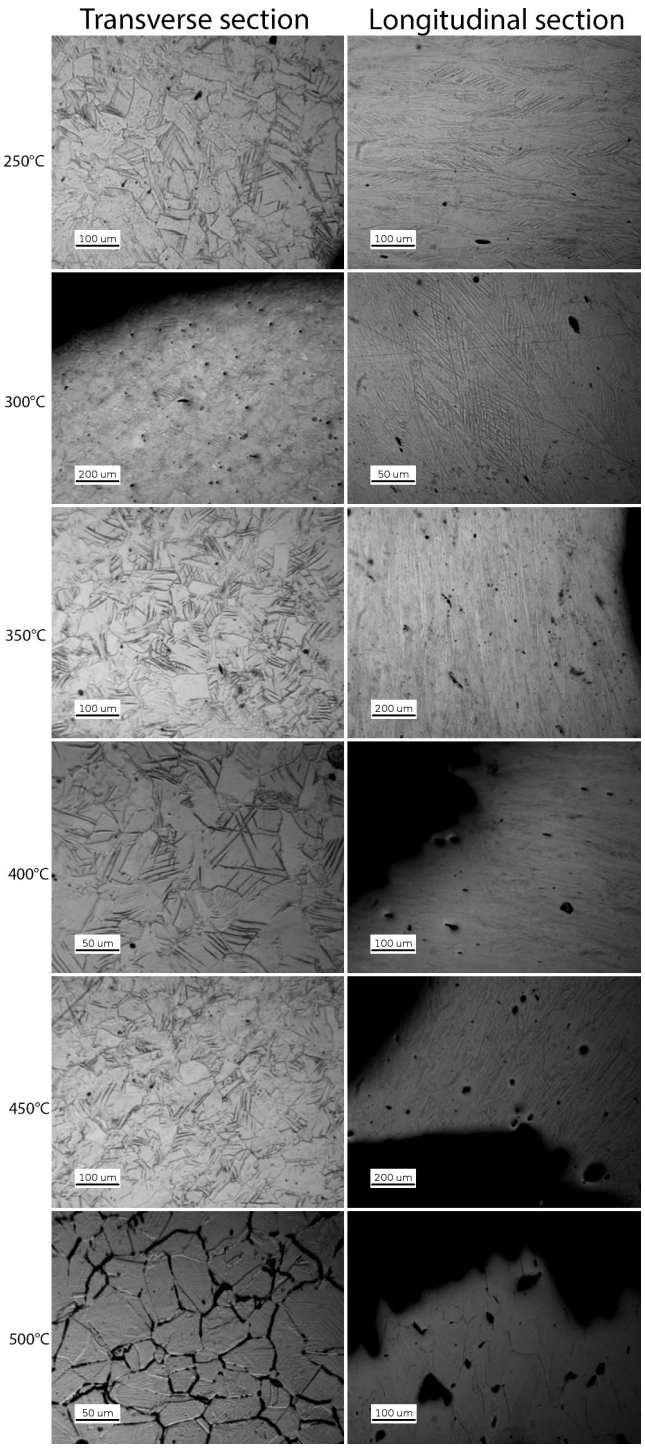

Fig. 5. Metallographic observations performed on the transverse and longitudinal section of the tested tensile specimens. The section aligned with the specimen axis has been observed near the developed fracture.

Table 5. Average grain size (equivalent diameter) measured on the transverse section of the specimens and detected percentage volume fraction of chromium carbides.

Temperature [°C]	250	300	350	400	450	500
Average grain size [μm]	105	107	113	127	139	157
Chromium carbides volume fraction [%]	0.02	0.03	0.03	0.04	0.06	0.75

mium carbides. The observed grain size increases as the plastic deformation temperature increases, while the volume fraction of the chromium carbides takes place mainly at 500°C.

The observations performed by STEM point out clearly that the dislocation density is higher in the steels deformed at the lowest temperature range (**Fig. 7**), while the specimens deformed at the highest temperature show a lower dislocation density and wide portions of the grains are not featured by the presence of a dislocation forest but they seem to be interested by the reorganization of the disloca-

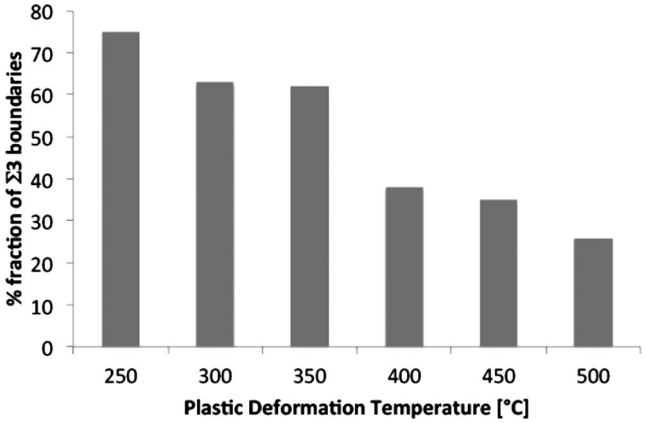

Fig. 6. Percentage fraction of Σ3 boundaries as a function of the applied plastic deformation temperature.

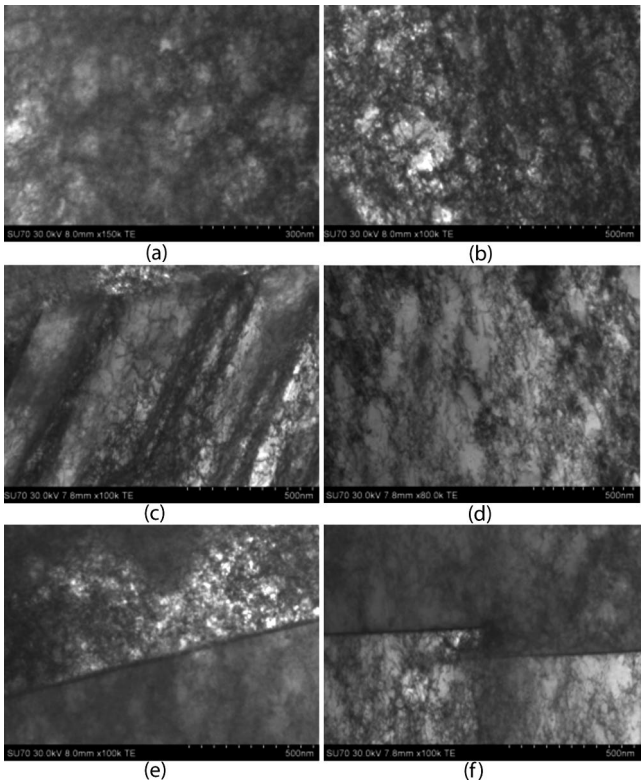

Fig. 7. STEM observation of the dislocation on the specimens treated at (a) 250°C, (b) 350°C, (c) 450°C, (d) 500°C and detail near the grain boundary for sample treated at (e) 350°C and (f) 500°C.

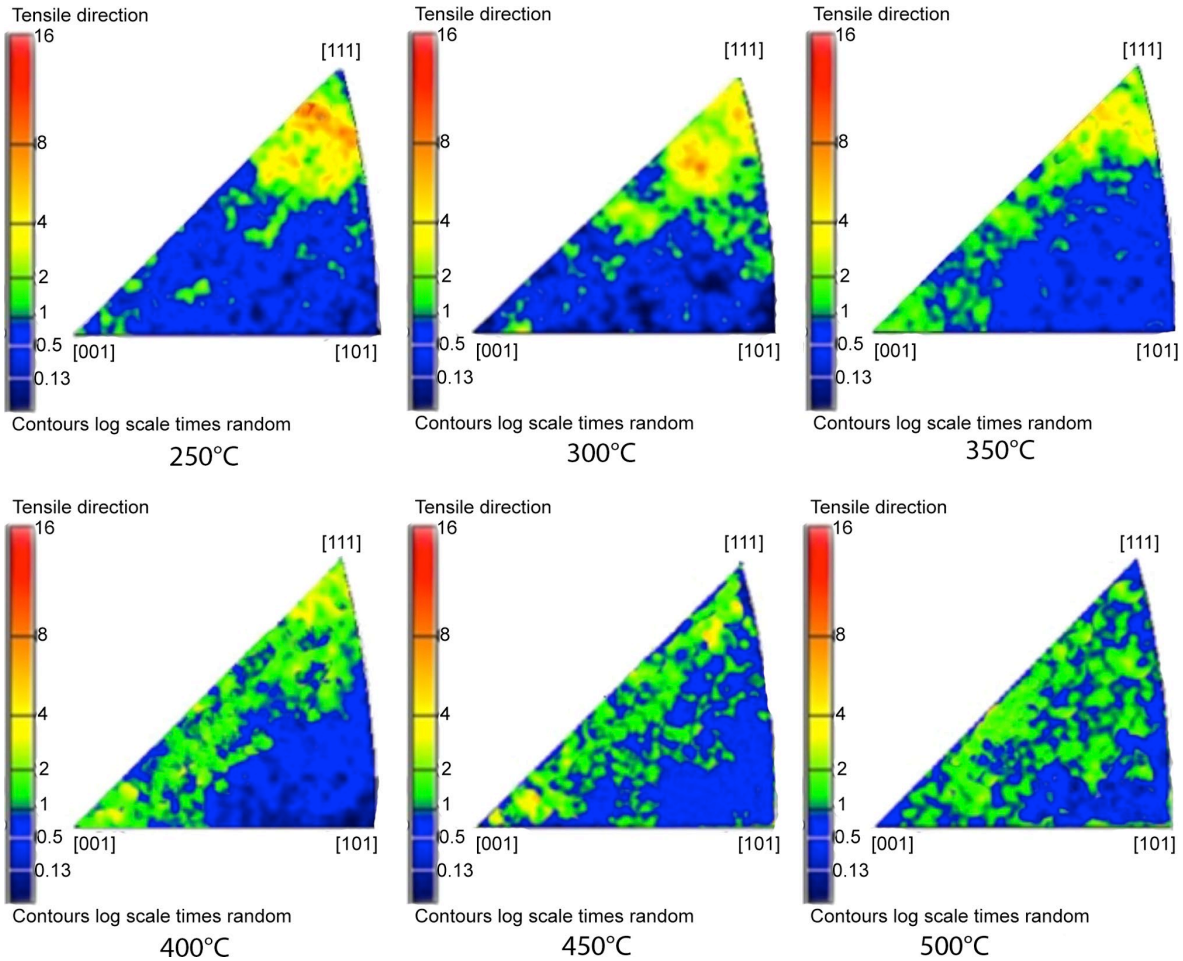

Fig. 8. Inverse pole figures of the specimens plastically strained at high temperature up top 23% deformation. (Online version in color.)

Table 6. Dislocation density (ρ_{disl}) revealed in the steel coupons strained at different test temperature up to 23% deformation.

Temperature [°C]	250	300	350	400	450	500
ρ_{disl} [m^{-2}]	$9.97 \cdot 10^{14}$	$1.05 \cdot 10^{15}$	$1.03 \cdot 10^{15}$	$9.7 \cdot 10^{14}$	$8.1 \cdot 10^{14}$	$2.7 \cdot 10^{14}$

tions along particular directions forming boundaries (**Fig. 8**). The measured dislocation density varies as a function of the deformation temperature (**Table 6**). Thus, the specimens treated at the highest temperature point out clear traces of recovery, while the specimens strained in the lowest thermal range (between 250°C and 350°C) show a typical strain hardened microstructure featured by a high dislocation density and the dislocations are more homogeneously distributed.

The texture investigations are presented under the form of inverse pole figures (Fig. 8), because the studied specimens have been strained along the tensile direction, so this representation is significant to point out the orientation assumed by the grains after the deformation at temperature higher than the room temperature. The specimens strained at the lowest temperatures show the formation of a clear texture featured by the alignment of the <111> direction of the crystal lattice along the tensile direction while the textures appear less intense as the test temperature increases, actually a very weak texture has been pointed out for the coupons are strained at 500°C. A clear trend has been pointed out: the lower the plastic deformation temperature, the stronger the alignment of the <111> direction of the crystal lattice along the tensile direction.

4. Discussion

The martensite is formed only at 250°C and this phenomenon excludes the possibility to perform the hardening process at this temperature or at a lower thermal range, because this phenomenon causes the presence of a magnetic permeability that has to be avoided.[10–12)]

The observed flow stresses of the studied steel during the tensile tests performed above the room temperature are featured by a decreasing trend as the temperature increases, but above 350°C also the overall elongation at the fracture point decreases as temperature increases. The specimens strained at 500°C is affected by a significant loss of ductility. Such an observed behavior is due to the abundant precipitation of the chromium carbides at the grain boundaries. The precipitation phenomena of the chromium carbides become evident at 500°C and it has to be avoided in order to prevent hot shortness of the steels and the consequent possible damages. The carbide precipitation and the consequent removal of the carbon from the metal lattice implies also a decreasing of the strain aging phenomenon that is evident in the tensile test realized at room temperature for the steels deformed at temperature lower than 500°C and this phenomenon points out that below 500°C the carbide precipitation decreases as the applied deformation temperature decreases.[13)]

The presence of martensite in the samples deformed at the lowest temperature (250°C) explains why their ductility is lower than the ductility observed for the samples deformed at 300°C and 350°C when the deformation is mainly realized by twinning as can be expected in austenite steels featured by a fcc elementary cell.[13–17)] The metallographic observations at room temperature performed on the specimens confirm that the twinning density (Figs. 7, 8) in the deformed grains decreases as the temperature increases (400°C–450°C–500°C). This is consistent also with the dislocation density identified by the STEM observations, through which the difference in terms of the dislocation distributions as a function of the deformation temperature is made evident. The lowest applied thermal range of deformation (250°C–300°C–350°C) causes the presence of a homogeneous dislocation density while the highest applied thermal range (400°C–450°C–500°C) implies a reorganization of the dislocation and wide portions of the alloy appear not interested by the presence of dislocations. This qualitative statement has been confirmed by the measured dislocation density (Table 6).

The SEM-EBSD measurement confirm this statement, because the anisotropy of the deformed specimens is weakened as the deformation temperature increases, because the recovery mechanism, the reorganization of the dislocation and the generation of sub-grains imply a more homogeneous distribution for the orientation of the crystal lattices.[18–21)]

The tensile tests performed at room temperature point out that the best mechanical properties are obtained for the specimens plastically deformed at the lowest temperature range, because the highest twinning and the highest dislocation density are maintained down to the room temperature and this situation improves the desired hardening effect. Actually, the strain hardening mechanism is improved by an increase of the dislocation density according to the Eq. (2):[8,22–24)]

$$\sigma = \alpha G |b| \sqrt{\rho_{disl}} \quad \text{..... (2)}$$

where α is a constant, G is the shear modulus of the steel, b is the length of the dislocation Burger vector and ρ_{disl} is the dislocation density.

Thus, if the specimens have been featured by the formation of a high dislocation density and the recovery mechanism does not take place, such situation allows exploiting also the "Suzuki" hardening effect[9)] taking place when the dislocations are dissociated. The stacking sequence in the regions of the stacking fault between the two partial dislocations is a thin region featured by hcp (hexagonal compact prism) crystal structure. The solubility of the alloying elements may be higher in the stacking fault than in the bulk lattice; as a result the solutes can segregate to the region interested by the stacking fault and so they can immobilize the partial dislocations and they can increase the hardening effect.

On the basis of the obtained results, the most suitable thermal range can be stated between 300°C and 350°C, because for a lower deformation temperature the martensite can form, while for temperature above this range the activation of a recovery mechanism weakens the hardening effect at room temperature. Actually, the coupons plastically deformed above 350°C are featured by a decreased dislocation density due to the occurrence of a recovery mechanism, while the strain hardening effect is increased in the samples featured by a high dislocation density maintained (after

the plastic deformation) down to the room temperature. At 500°C the softening due the dislocation recovery mechanism is associated even to a very detrimental precipitation of the chromium carbides that negatively affects the strength properties of the steel at room temperature.

5. Conclusions

The carried out experimental activities aim at understanding the best temperature range to perform the plastic deformation of the steel X10CrMnN18-18 in order to achieve a hardening that allows to obtain the high strength required for the realization of high strength components, *i.e.* retaining rings:

- the best combination of the usually required mechanical properties at room temperature (Table 4) can be achieved after a deformation realized between 250°C and 350°C, while after a plastic deformation performed at 400°C the mechanical properties are very near the lowest required limits;
- a hardening procedure performed at temperature higher than 450°C causes clear recovery phenomena and a significant intergranular precipitation of the chromium carbides that eliminates the strain aging at the yield point, but the removal of carbon and chromium from the metal matrix does not allow exploiting the solution strengthening and the "Suzuki" effect which cover a fundamental role for achieving the required high strengths;
- the work hardening procedure performed between 250°C and 350°C induces the highest dislocation density at room temperature, while as the temperature increases over such a thermal range, the recovery phenomena take place and this implies a coarsening of the grains, a consequent decrease of the strengthening properties (YS, UTS) and an increase of the ductility at room temperature;
- thus, the optimal thermal range for the application of the plastic deformation has to be set between 300°C and 350°C, in order to harden the steel by the increase of the dislocation density as well as by the formation of martensite.

REFERENCES

1) C. Scott, S. Allain, M. Faral and N. Guelton: *Rev. Metall.*, **103-6** (2006), 293.
2) A. I. Z. Farahat, O. Hamed, A. El-Sisi and M. Hawash: *Mater. Sci. Eng. A-Struct*., **530** (2011), 98.
3) S. R. Kalidindi: *Int. J. Plast.*, **14** (1998), 1265.
4) J. A. Jimenez and G. Frommeyer: *Mater. Charact.*, **61** (2010), 221.
5) G. Saller, H. Aigner, M. O. Speidel, C. Kowanda and M. Diener: Proc. HNS 2003, vdf Hochschulverlag, Zurich, (2003), 341.
6) J. N. Bernauer and G. Saller: *Trans. Ind. Inst. Met.*, **55** (2002), 193.
7) G. Stein, J. Menzel, M. O. Speidel and P. J. Uggowitzer: Ergebnisse der Werkstoff-Forschung, Band 4, Stickstofflegierte Stahle, Thubal-Kain, Zurich, (1991), 33.
8) B. C. De Cooman, J. G. Speer, I. Y. Pyshmintsev and N. Yoshinaga: Materials Design – The key to modern steel products, Grips Media, Bad Harzburg, Germany, (2007), 277.
9) B. C. De Cooman, J. G. Speer, I. Y. Pyshmintsev and N. Yoshinaga: Materials Design – The key to modern steel products, Grips Media, Bad Harzburg, Germany, (2007), 270.
10) I. Solomon and N. Solomon: *Rev. Metal. Madrid*, **46** (2010), 121.
11) I. Meszaros and J. Prohaszka: *J. Mater. Process. Technol.*, **161** (2005), 162.
12) H. Ishigaki, Y. Konishi, I. Kondo and K. Koterazawa: *J. Magn. Magn. Mater.*, **193** (1999), 466.
13) W. S. Owen and M. Grujicic: *Acta Mater.*, **47** (1999), 111.
14) P. J. Uggowitzer, M. O. Speidel and P. J. Uggowitzer: Ergebnisse der Werkstoff-Forschung, Band 4: Stickstofflegierte Stahle, Thubal-Kain, Zurich, (1991), 87.
15) P. Mullner, C. Solenthaler, P. Uggowitzer and M. O. Speidel: *Mater. Sci. Eng. A-Struct*., **164** (1993), 164.
16) H. E. Hanninen, N. Akdut, B. C. Cooman and J. Foct: Proc. HNS 2004, GRIPS media, Bad Harzburg, Germany, (2004), 371.
17) A. S. Hamada, L. P. Karjalainen, R. D. K. Misra and J. Talonen: *Mater. Sci. Eng. A-Struct*., **559** (2013), 336.
18) Y. Ding, J. Jiang and A. Shan: *J. Alloy. Compd.*, **487** (2009), 517.
19) W. Oliferuk and M. Maj: *Mater. Sci. Eng. A-Struct*., **462** (2007), 363.
20) T. S. Byun, N. Hashimoto and K. Farrell: *Acta Mater.*, **52** (2004), 3889.
21) G. Saller, K. Spiradek-Hahn, C. Scheu and H. Clemens: *Mater. Sci. Eng. A-Struct*., **427** (2006), 246.
22) A. S. Hamada and L. P. Karjalainen: *Mater. Sci. Eng. A-Struct*., **527** (2010), 5715.
23) F. de las Cuevas, M. Reis, A. Ferraiuolo, G. Pratolongo, L. P. Karjalainen, J. Alkorta and J. Gil Sevillano: *Key Eng. Mater.,* **423** (2010), 147.
24) R. D. K. Misra, P. K. C. Venkatsurya, M. C. Somani and L. P. Karjalainen: *Metall. Mater. Trans. A*, **43** (2012), 5286.